Supporting Information for

Remarkable Gas Adsorption by Carbonized Nitrogen-Rich Hypercrosslinked Porous Organic Polymers

Xiao Yang, Miao Yu, Yang Zhao, Chong Zhang, Xiaoyan Wang, Jia-Xing Jiang*

School of Materials Science and Engineering, Shaanxi Normal University, Xi'an, 710062, Shaanxi, P. R. China

E-mail: jiaxing@snnu.edu.cn

Table of Contents

Table S1. Yield and elemental analysis for the carbon materials

Sample	Yield (%)	C (%)	H (%)	N (%)
FCDTPA	95.04	89.29	5.81	4.90
FCDTPA-500	68.50	91.21	3.97	4.82
FCDTPA-700	38.24	93.14	2.15	4.71
FCDTPA-900	24.41	96.92	1.70	1.38
FCDTPA-K-500	62.85	90.58	4.72	4.70
FCDTPA-K-700	35.12	95.43	2.21	2.36
FCDTPA-K-900	21.22	97.53	1.08	1.39

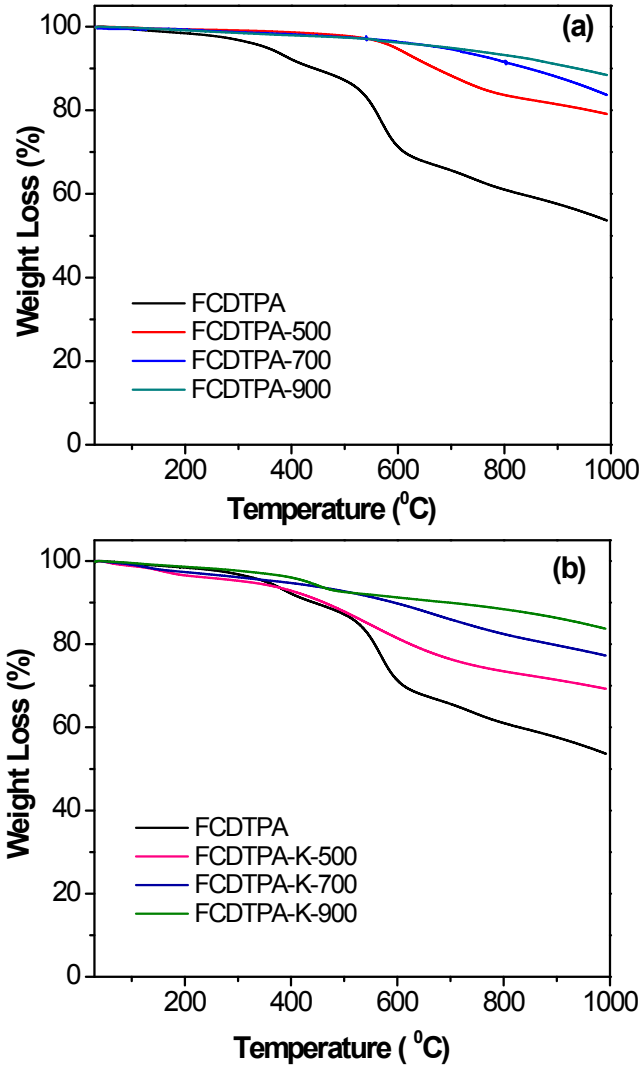

Figure S1. Thermogravimetric analysis curves for the direct carbonization materials (a), and the KOH-activated carbon materials (b) under a nitrogen atmosphere with a heating rate of 10 °C /min.

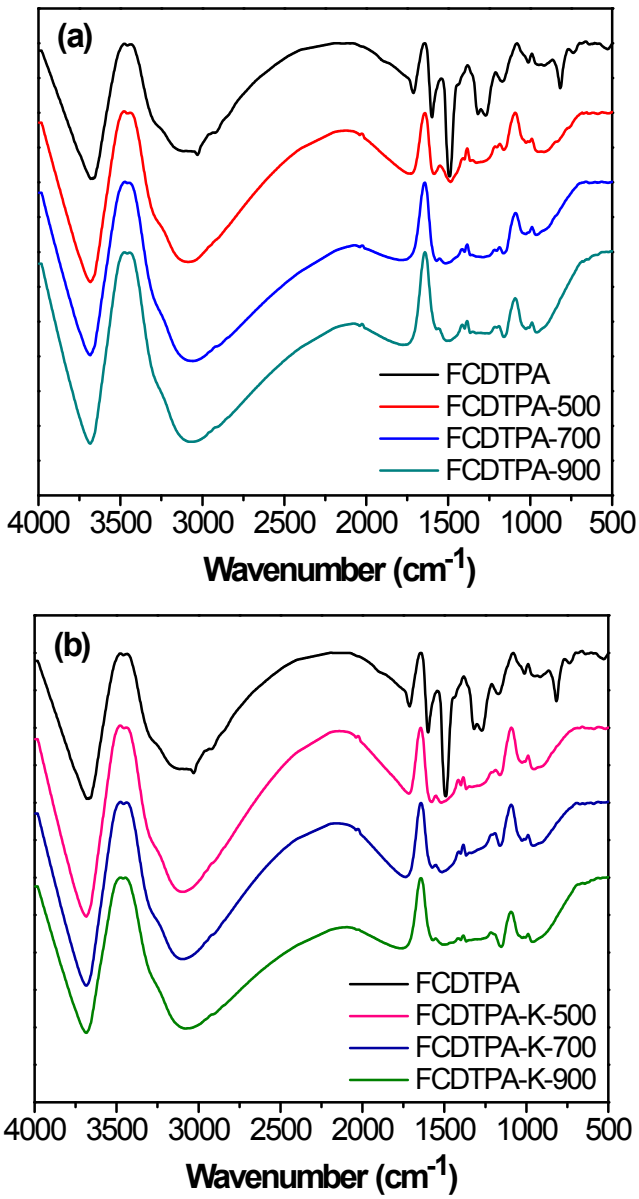

Figure S2. FT-IR spectra for the direct carbonization materials (a), and the KOH-activated carbon materials (b) using KBr disk.

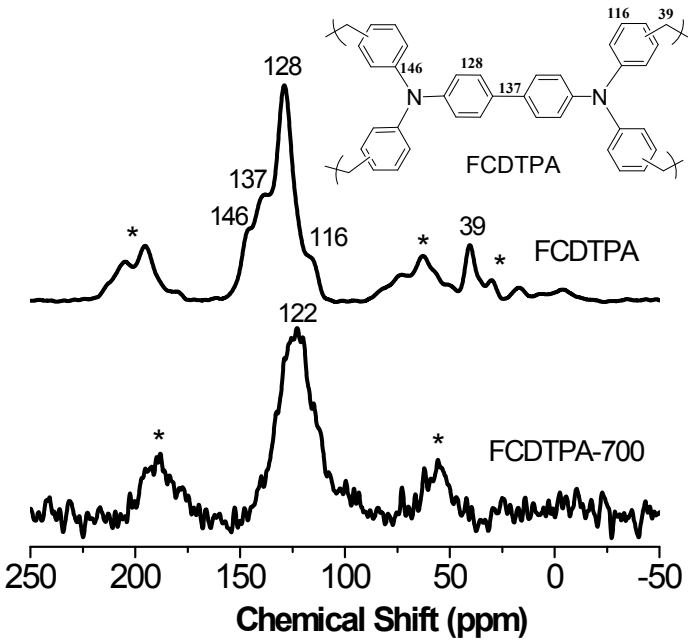

Figure S3. Solid state ^{13}C CP/MAS NMR spectra of FCDTPA and an example (FCDTPA-700) for the carbonized materials; asterisks denote spinning sidebands. The strong signals in the range of 116–146 ppm from the aromatic carbon atoms were observed in the ^{13}C CP/MAS NMR spectrum for the precursor of FCDTPA. The signal peak at 146 ppm corresponds to the substituted phenyl carbons binding with nitrogen atom. The signal peak at 137 ppm is ascribed to the substituted phenyl carbons. The signal peak for the unsubstituted phenyl carbons is located at 128 and 116 ppm, respectively. The signal near 39 ppm is related to the methylene carbon atoms, indicating that the fromaldehyde dimethyl acetal (FDA) participated in the polymerization. As a sharp contrast, the solid state ^{13}C CP/MAS NMR spectrum of FCDTPA-700 shows only one broad signal peak at around 122 ppm, indicating that the precursor was successfully converted to carbon materials.

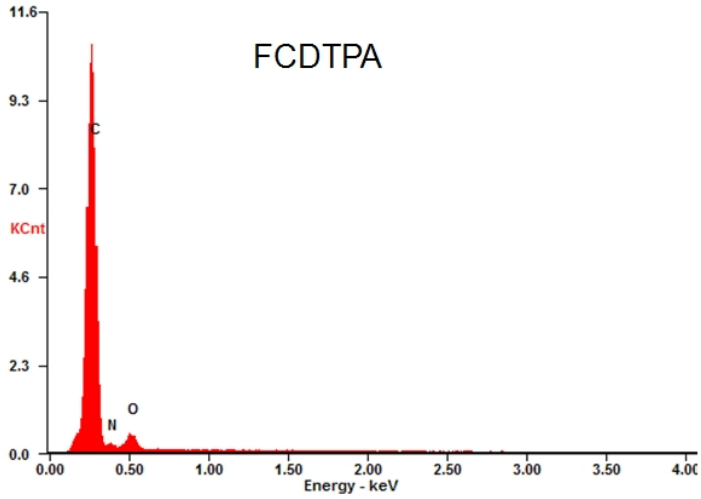

Figure S4. Energy dispersive X-ray spectroscopy spectrum of the precursor of FCDTPA.

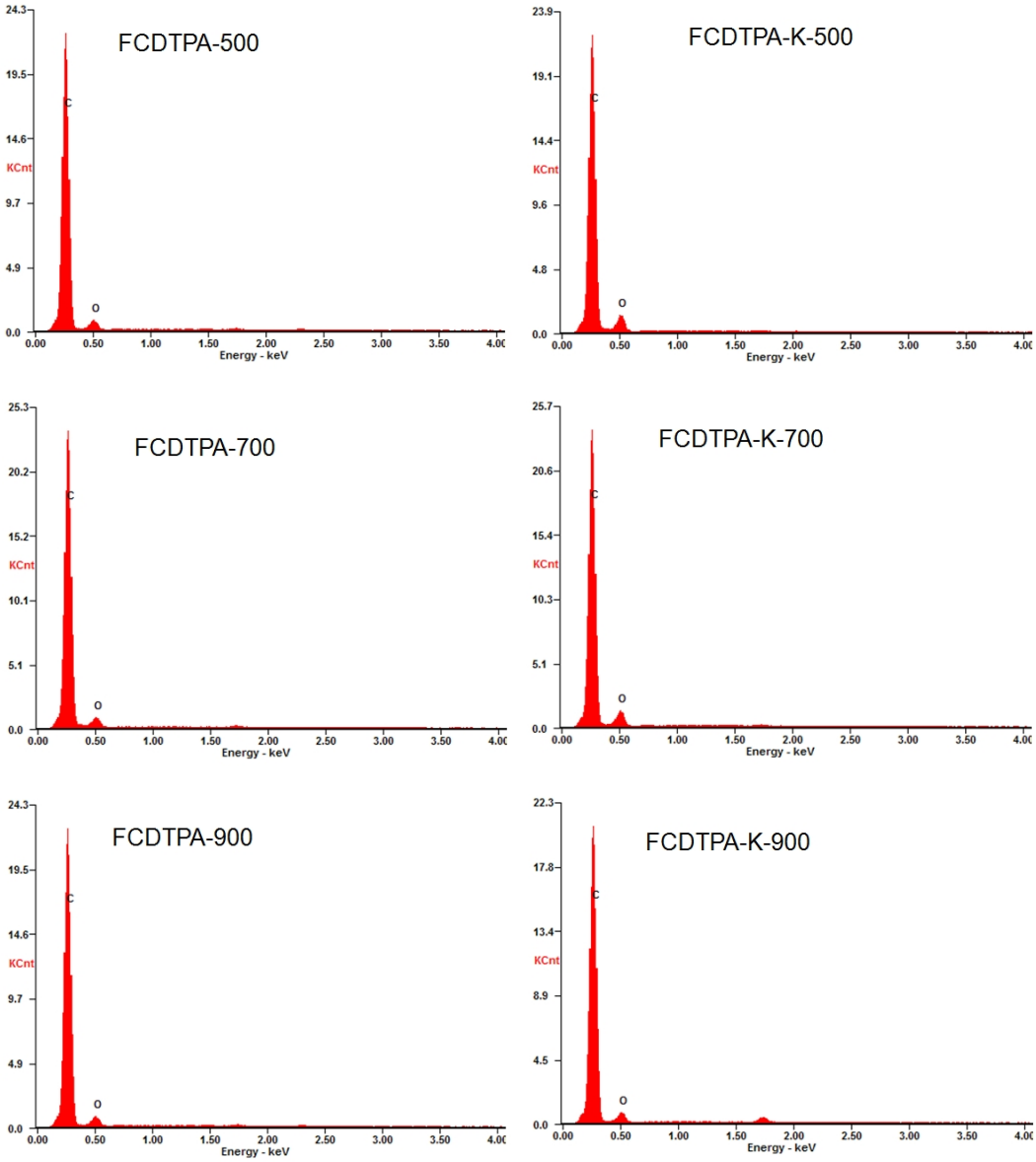

Figure S5. Energy dispersive X-ray spectroscopy spectra of the carbon materials.

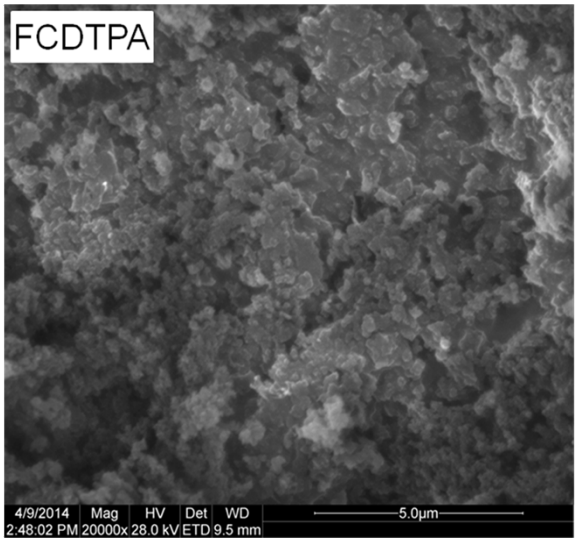

Figure S6. Scanning electron microscopy image for the precursor of FCDTPA.

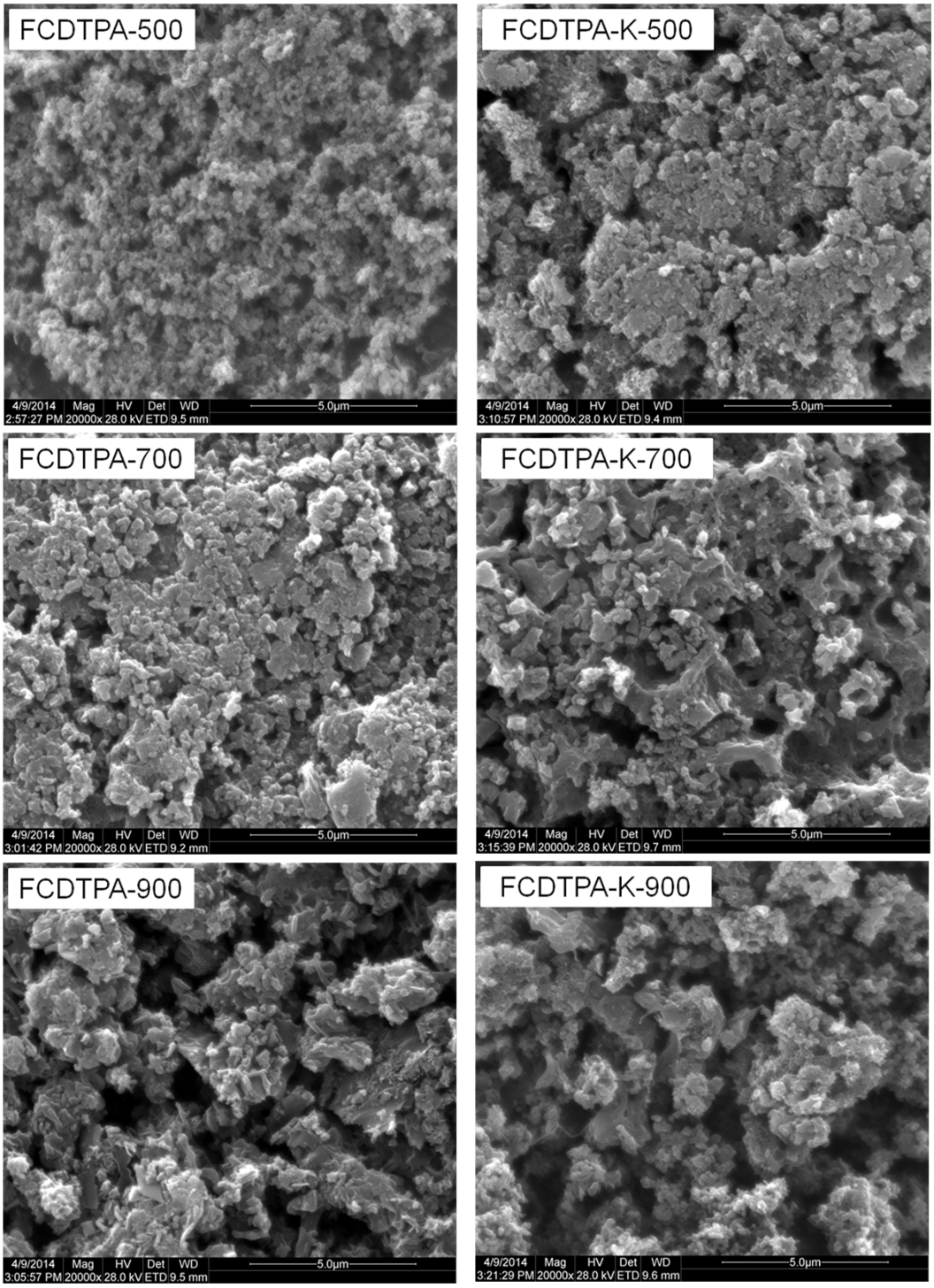

Figure S7. Scanning electron microscopy images for the carbon materials with a scale bar of 5.0 μm.

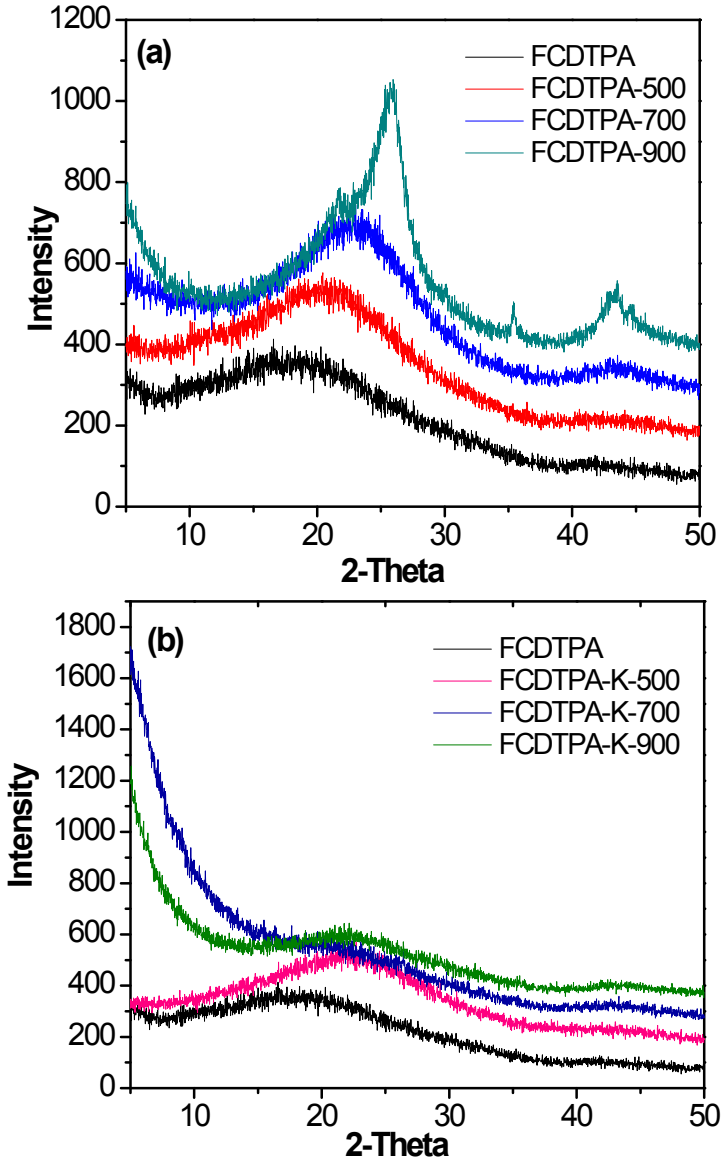

Figure S8. Powder XRD patterns for the direct carbonization materials (a), and the KOH-activated carbon materials (b).

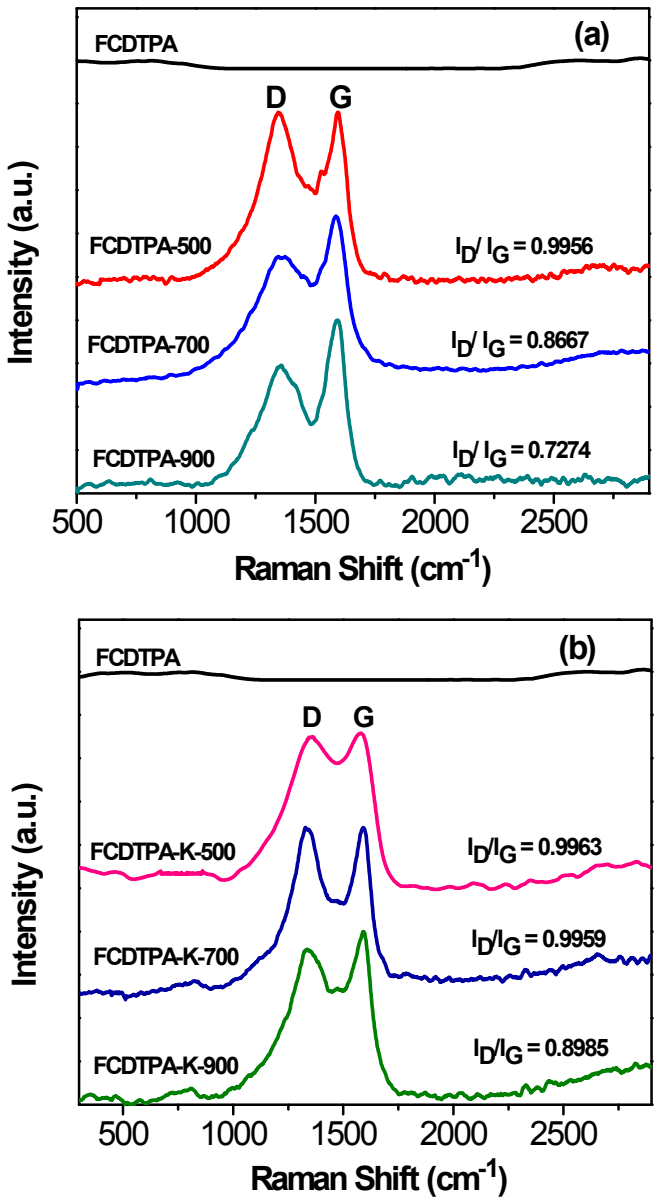

Figure S9. Raman spectra for the direct carbonization materials (a), and the KOH-activated carbon materials (b).

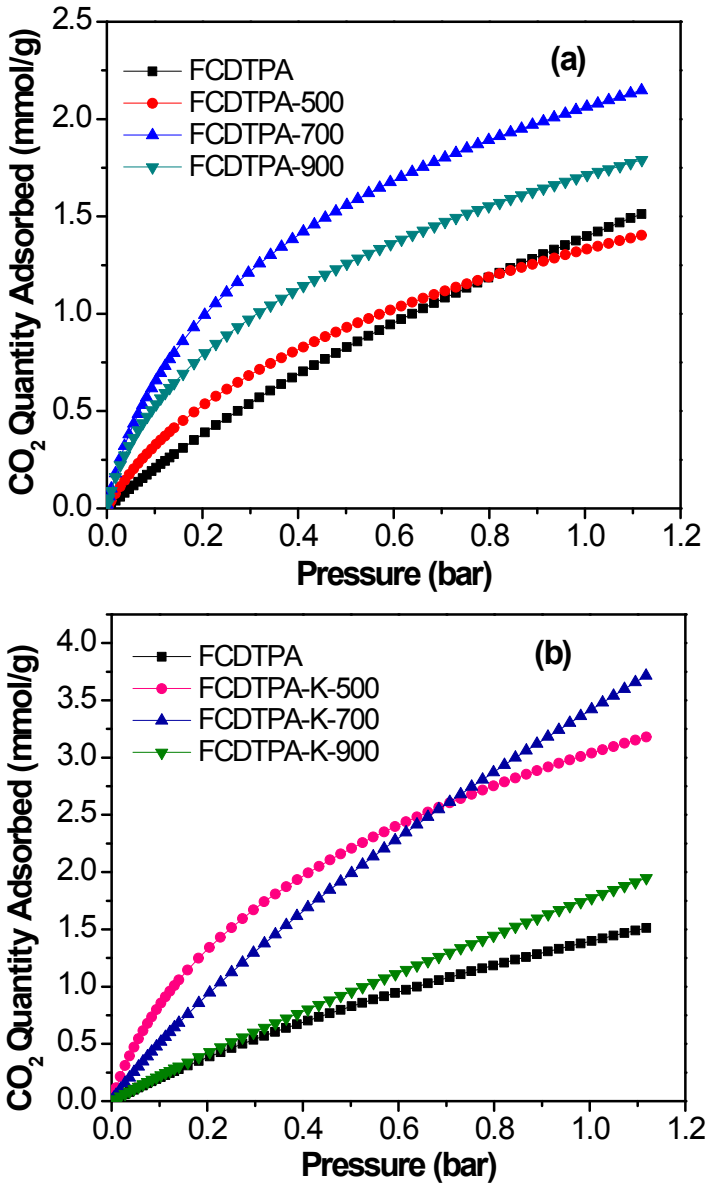

Figure S10. CO_2 adsorption isotherms of the direct carbonization materials (a), and the KOH-activated carbon materials (b) collected at 298 K.

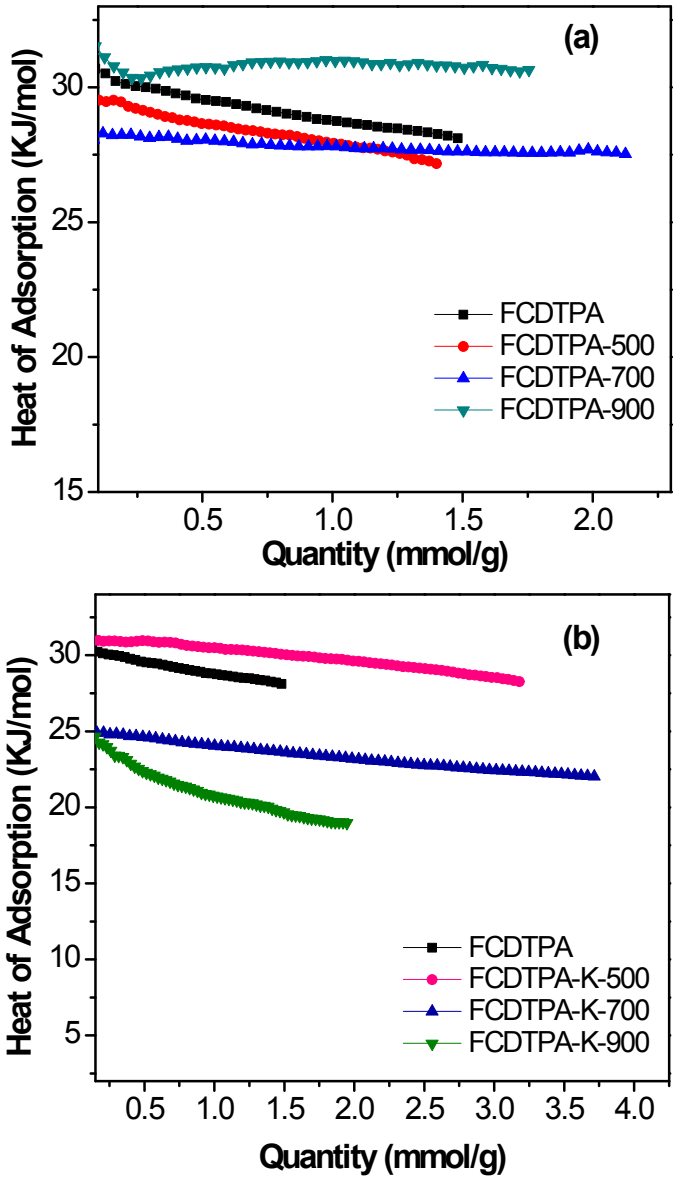

Figure S11. Isosteric heats of CO_2 adsorption for the direct carbonization materials (a), and the KOH-activated carbon materials (b) calculated from the adsorption isotherms collected at 273 and 298 K, respectively.

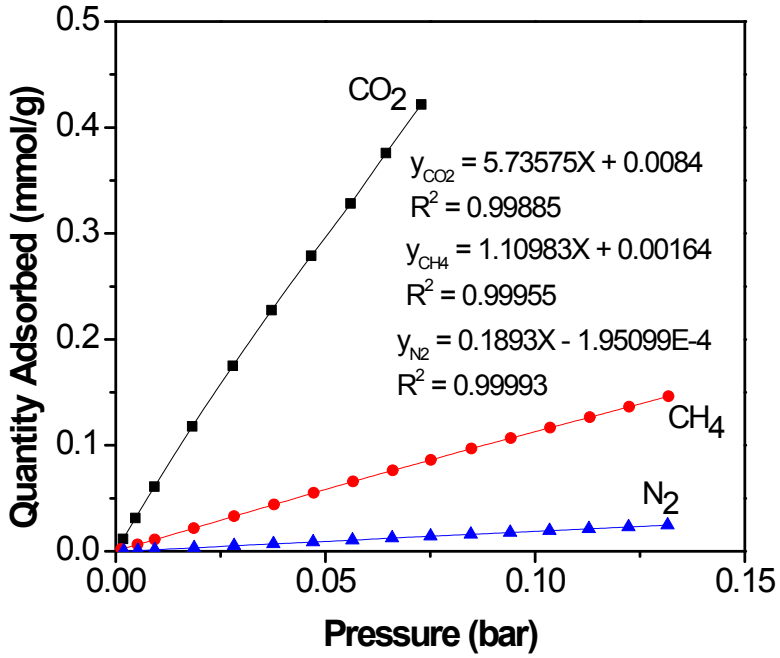

Figure S12. Gas adsorption selectivity for the precursor of FCDTPA using the ratios of the Henry law constant calculated from the initial slopes of the single-component gas adsorption isotherms collected at low pressure coverage (< 0.15 bar) and 273 K.

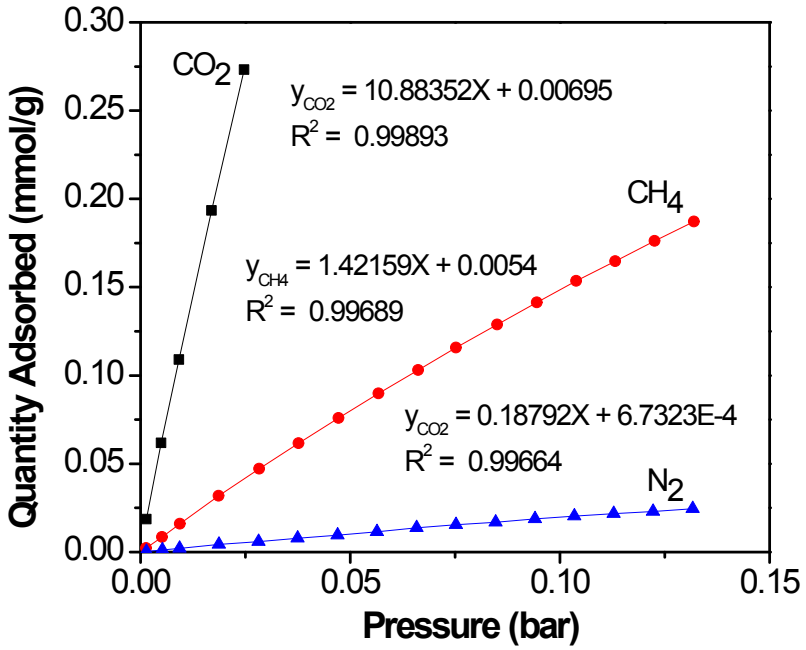

Figure S13. Gas adsorption selectivity for the FCDTPA-500 using the ratios of the Henry law constant calculated from the initial slopes of the single-component gas adsorption isotherms collected at low pressure coverage (< 0.15 bar) and 273 K.

.

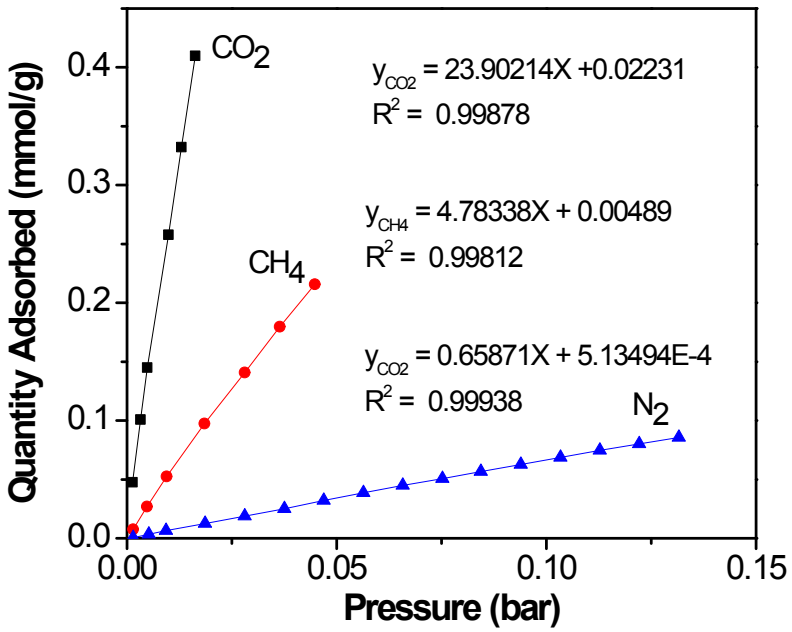

Figure S14. Gas adsorption selectivity for the FCDTPA-700 using the ratios of the Henry law constant calculated from the initial slopes of the single-component gas adsorption isotherms collected at low pressure coverage (< 0.15 bar) and 273 K.

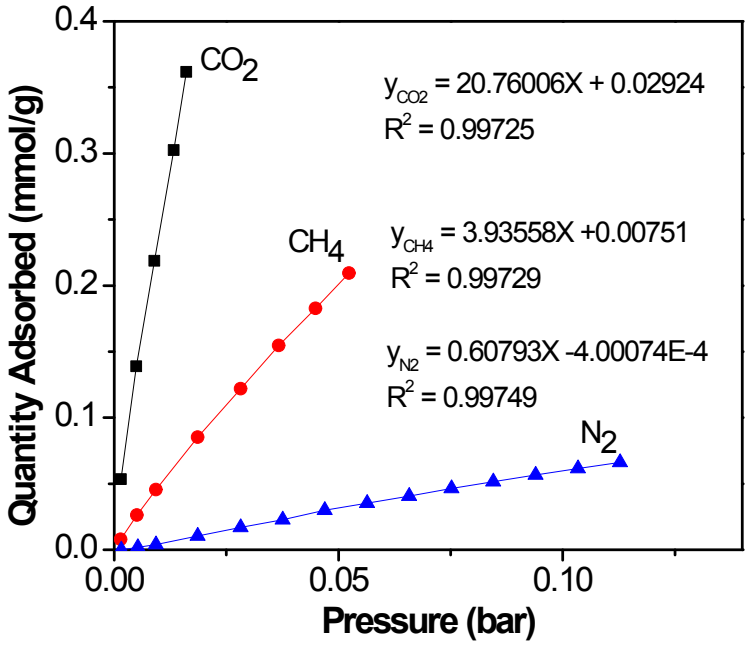

Figure S15. Gas adsorption selectivity for the FCDTPA-900 using the ratios of the Henry law constant calculated from the initial slopes of the single-component gas adsorption isotherms collected at low pressure coverage (< 0.15 bar) and 273 K.

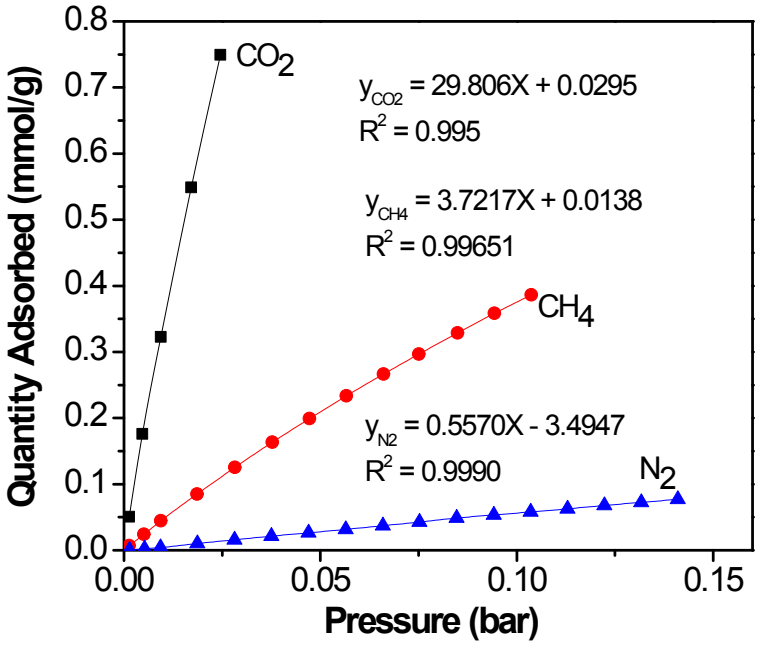

Figure S16. Gas adsorption selectivity for the FCDTPA-K-500 using the ratios of the Henry law constant calculated from the initial slopes of the single-component gas adsorption isotherms collected at low pressure coverage (< 0.15 bar) and 273 K.

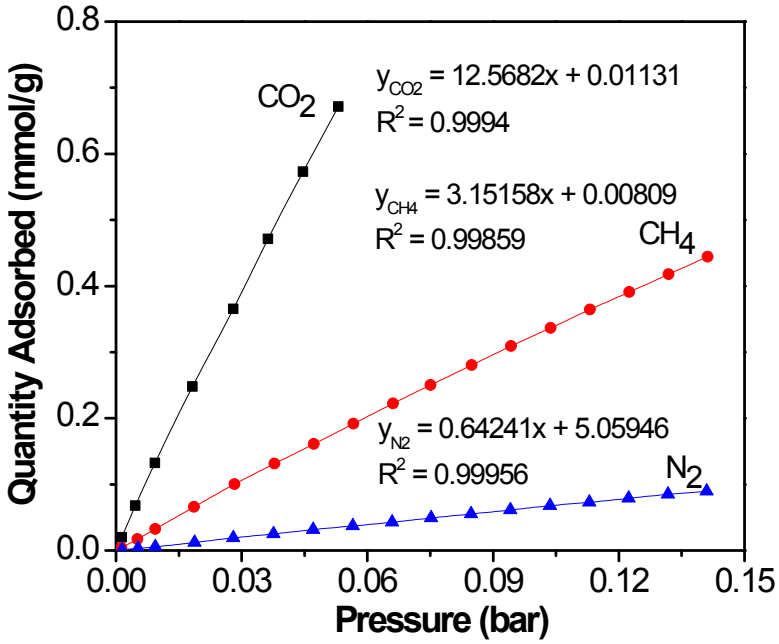

Figure S17. Gas adsorption selectivity for the FCDTPA-K-700 using the ratios of the Henry law constant calculated from the initial slopes of the single-component gas adsorption isotherms collected at low pressure coverage (< 0.15 bar) and 273 K.

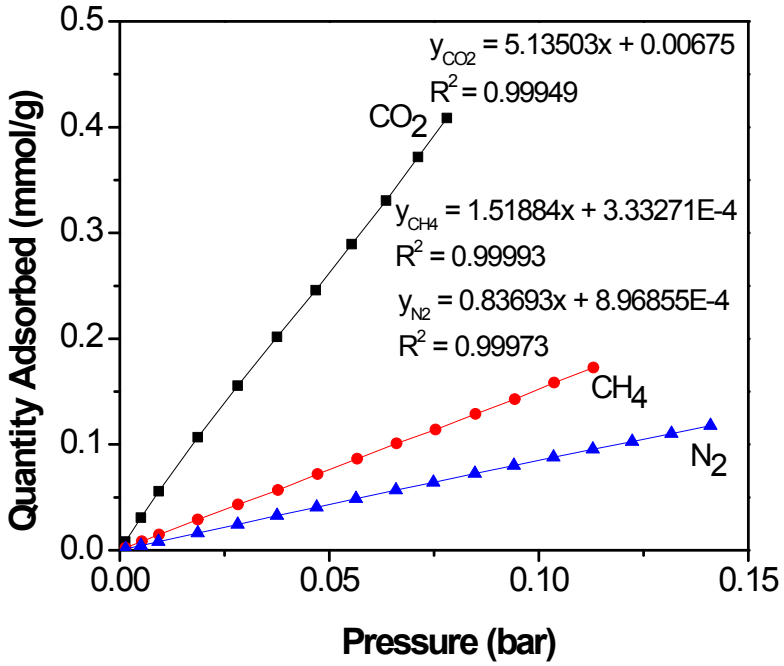

Figure S18. Gas adsorption selectivity for the FCDTPA-K-900 using the ratios of the Henry law constant calculated from the initial slopes of the single-component gas adsorption isotherms collected at low pressure coverage (< 0.15 bar) and 273 K.